

Knowing - How on Boundary Geometric Moments

Javier Montenegro Joo

Virtual Dynamics / Virtual Labs: Science & Engineering, Calle 14-572, Las Magnolias de Surco, Lima 33, Perú

ABSTRACT .-In this research the performance of the Chen's Improved (Boundary) Moments is carefully compared to that of the traditional (Massive) Moments, to achieve this investigation, the pattern recognition power of the former is thoroughly assessed against that of the latter. The boundary moments are evaluated by two methods, in the first by edge-tracing, in the second method the edge pixels are considered as they are met when sweeping the image space. It is found that the boundary moments produce the same numerical values with the two methods. It is also found that the average "distance" between a reference and trial samples for massive and boundary moments yield approximate values, implying that these two methods are equivalent concerning accurateness.

It is concluded that the computation of the Boundary Moments by sweeping the image space associates minimum computational complexity to a high enough object classification efficiency, thus they may be used in lieu of the traditional moments.

The research includes hollowed objects, it is experimentally demonstrated that pattern classification of this kind of objects can also be successfully achieved with the boundary moments, provided that they are evaluated by sweeping the image space.

I. INTRODUCTION

The (Massive) Moment Invariants, a powerful tool to execute invariant pattern recognition of objects were introduced at the beginning of the sixties by M.K. Hu [1,2], these traditional invariants need the coordinates of all the bidimensional object pixels in image space in order to be computed. Following Hu, many papers have appeared dealing with shortcut ways to compute those massive moments. In 1993, C.C. Chen [3] introduced the Improved Moment Invariants, this is a reformulation of Hu's moments and they are a set of invariants devised in such a way as to be evaluated only with the object boundary pixels. The author of the

present paper [4] has pointed out that Chen's discretized equations do not specify any particular pixel sequence to be followed in the computations, this means that there is no need to use any boundary chain code representation, as suggested by Chen [3].

On the other hand it seems obvious that if these improved moments have been devised for the object edge, then they must be computed by regarding the edge as an ordered chain of pixels (edge-tracing) and not as a chunk of pixels (when the pixels are taken into account by simply sweeping the image space, they are being considered as a chunk of pixels). It is to overcome this ambiguity that a comparative study of Chen's moments by two methods of evaluating them was carried out having as a reference Hu's moments. The study was accomplished in order to gather information about Chen's moments performance so as to know which method results more efficient in terms of accurateness and computer complexity.

The research being reported here evaluated the massive moments as usual by simply sweeping the image space and taking the object pixels as these were met, for the evaluation of the Improved or Boundary Moments, after object edge-detection two methods were investigated, in the first, the boundary pixels were considered while walking along the object boundary, this is edge-tracing; in the second method, the image space was swept and the boundary pixels were considered as they were met, this is, they were regarded as a chunk of pixels.

Concerning the organization of this paper, in the following section a glance over some previous related works show that boundary-like moments were usually computed by edge-tracing. Then the massive and the boundary moments are quickly reviewed in two separate sections. A description of the experiments carried out is next, some tables showing experimental results and some of the objects used are displayed. Finally a section devoted to discussion and another to the conclusions is presented.

Hereafter, RTS will stand for rotation, translation and size-scaling.

II. SOME PREVIOUS RELATED WORKS

After the works of Hu [1,2] several attempts have been made to reduce the computation complexity involved in the calculation of the invariant moments. From all these, some attempted to work only with the object boundary, among these works there is the one of Li and Sheng [5] whose method requires pixel-by-pixel summations along the object contour in an ordered way.

The work of Singer [6] is based on a polygonal approximation of the object and a list of neighbouring pixels.

Jiang and Bunke [7] report using the Green's theorem to shift from an area integral to a line integral. Their method requires a counterclockwise direction list of the border pixels.

Jia-Guu Leu [8] uses a series of triangles to compute the object moments, this method requires a list of the object polygonal approximation vertices in clockwise direction.

Dudani et al [9] carried out moment invariant computations over both, object body and contour, using a normalization factor different to that of the type originally proposed by Hu. In the case of contour moments these authors do not specify whether they are performed by edge-tracing or image-space sweeping.

Mingfa et al [10] computes boundary moments after applying a boundary-tracing algorithm.

Fu et al [11] apply some pre-processing to obtain the object edge and trace the boundary curve clockwise, then these authors use the Hadamard transformation to compute the moment invariants.

Wen and Lozzi [12] compute line moments of object boundaries. They consider object polygonal approximations and their method requires a list of the polygon vertices so as to compute the moments of each linear segment.

As it can be seen the above mentioned attempts to compute the boundary moments have all included some sort of edge-tracing. Even though those works are proposing alternative methods to evaluate Hu's traditional moments, they do not provide any experimental data so as to compare their recognition performance with that of Hu's method, they are rather concerned with the computer complexity and computational cost of the algorithms involved. The results of the research [4] being reported in this paper lead to the conclusion that if applying the Chen's improved moments it is more convenient to simply sweep the image space and to consider the object pixels as they are met, instead of carrying out edge tracing.

III. THE M. K. HU'S TRADITIONAL (MASSIVE) INVARIANT MOMENTS

In this section, a brief review of the Hu's invariant moments is presented. The two-dimensional traditional Geometric Moments of order $p+q$ of a density distribution (intensity function) $f(x, y)$ are defined as

$$m_{pq} = \int_{-\infty}^{+\infty} \int_{-\infty}^{+\infty} x^p y^q f(x, y) dx dy, \quad p, q = 0, 1, 2, \dots \quad (1)$$

and they are not invariant. The double integrals are to be considered over the whole area of the object including its boundary, this implies computational complexity of order $O(N^2)$. The density distribution function $f(x, y)$ gives the intensity color of the point (x, y) in image space. In practical pattern recognition applications the image space is reduced to a binary version, and in such a case $f(x, y)$ takes the value of 1 when the pixel (x, y) represents objects or even noise and it is 0 when it is part of the background.

When the geometrical moments m_{pq} in equation (1) are referred to the object centroid (x_c, y_c) they become the Central Moments, and are given by:

$$\mu_{pq} = \int_{-\infty}^{+\infty} \int_{-\infty}^{+\infty} (x-x_c)^p (y-y_c)^q f(x, y) dx dy \quad (2)$$

where $x_c = m_{10} / m_{00}$ and $y_c = m_{01} / m_{00}$.

The total area of the object is given by m_{00} and the

Central Moments μ_{pq} are invariant to translation and may be normalized to turn also invariant to area scaling through the relation:

$$\eta_{pq} = \frac{\mu_{pq}}{\mu_{00}^\gamma} \quad \gamma = \frac{p+q}{2} + 1 \quad (3)$$

The set of seven lowest order RTS invariant functions ϕ_i include invariants up to the third order, it is given by:

$$\phi_1 = \eta_{20} + \eta_{02}$$

$$\phi_2 = (\eta_{20} - \eta_{02})^2 + 4\eta_{11}^2$$

$$\phi_3 = (\eta_{30} - 3\eta_{12})^2 + (3\eta_{21} - \eta_{03})^2$$

$$\phi_4 = (\eta_{30} + \eta_{12})^2 + (\eta_{21} + \eta_{03})^2$$

$$\phi_5 = (\eta_{30} - 3\eta_{12})(\eta_{30} + \eta_{12})[(\eta_{30} + \eta_{12})^2 - 3(\eta_{21} + \eta_{03})^2] + (3\eta_{21} - \eta_{03})(\eta_{21} + \eta_{03})[3(\eta_{30} + \eta_{12})^2 - (\eta_{21} + \eta_{03})^2]$$

$$\phi_6 = (\eta_{20} - \eta_{02})[(\eta_{30} + \eta_{12})^2 - (\eta_{21} + \eta_{03})^2] + 4\eta_{11}(\eta_{30} + \eta_{12})(\eta_{21} + \eta_{03})$$

$$\phi_7 = (3\eta_{21} - \eta_{03})(\eta_{30} + \eta_{12})[(\eta_{30} + \eta_{12})^2 - 3(\eta_{21} + \eta_{03})^2] - (\eta_{30} - 3\eta_{12})(\eta_{21} + \eta_{03})[3(\eta_{30} + \eta_{12})^2 - (\eta_{21} + \eta_{03})^2]$$

in practical pattern recognition applications the equations (1) and (2) are discretized for binary images according to

$$m_{pq} = \sum_x \sum_y f(x, y) x^p y^q \quad (5)$$

$$\mu_{pq} = \sum_x \sum_y f(x, y) (x - x_c)^p (y - y_c)^q \quad (6)$$

where m_{pq} and μ_{pq} are computed by sweeping the image space.

IV. THE C.C. CHEN'S IMPROVED (BOUNDARY) MOMENTS

Here the Boundary Moments are quickly reviewed. The paper of C.C. Chen [3] introduces a method to compute a set of slightly different invariant functions based on computations only along the boundary of the object. In this way the computational complexity of the problem and the computer time are reduced from $O(N^2)$ to $O(N)$. In his work, C.C. Chen uses the same RTS invariant functions given by equations (4) deduced originally by Hu, however he introduces a new scaling factor α instead of γ (see equations (12) and (3)) to achieve invariance to boundary length scaling.

The Chen's boundary geometrical moments are given by:

$$m_{pq} = \int_C f(x, y) x^p y^q dl \quad p, q = 0, 1, 2, \dots \quad (7)$$

where the integral is to be evaluated along the object edge C.

Discretizing equation (7), m_{pq} results in

$$m_{pq} = \sum_{(x,y) \in C} f(x, y) x^p y^q \quad (8)$$

As usual the coordinates of the object centroid (x_c, y_c) are given by:

$$(x_c, y_c) = \frac{1}{m_{00}} (m_{10}, m_{01}) \quad (9)$$

notice that m_{00} is in this case the length of the curve C, the edge of the object.

The boundary central moments --invariant to translation-- are given by:

$$\mu_{pq} = \int_C f(x, y) (x - x_c)^p (y - y_c)^q dl \quad (10)$$

and the integral must be evaluated along the boundary C of the object. In the discrete case μ_{pq} above becomes

$$\mu_{pq} = \sum_{(x,y) \in C} f(x, y) (x - x_c)^p (y - y_c)^q \quad (11)$$

and it can be seen that after discretization it is not necessary to carry out the sum in any particular order; this means that $(x, y) \in C$ can be taken in any order, for example, as they are met when sweeping the image space top-down and left-right.

The C.C. Chen's scale normalized central moments are given by:

$$\eta_{pq} = \frac{\mu_{pq}}{\mu_{00}^\alpha} \quad \alpha = p+q+1 \quad p+q=2, 3, \dots \quad (12)$$

here μ_{00} is the length of C. The η_{pq} are scale and translation invariant.

V. THE INVESTIGATION

In the investigation reported in this paper, 16 computer synthesized objects ($N_o = 16$) (see figures 1 and 2) were used, each one was randomly sampled in 6 different RTS versions ($N_s = 6$) and after computing the seven invariants (see equations (4)) of every sample s , a point in the Invariants Coordinate Space was obtained. For every object n the distances d_s ($s = 1, 2, 3, \dots, N_s - 1$) between its first sample invariant-space coordinates and the coordinates of the other 5 samples was

computed, where the first sample was taken as a reference. Then the mean distance $\langle d \rangle_n, n = 1, 2, \dots, N_o$ was calculated for every object as the mean d_s . This process was repeated for each one of the three methods studied.

Each object sample, this is every object RTS version, describes a point in the invariants hepta-dimensional space of coordinates $\phi_i, i = 1, 2, \dots, 7$. The distance d_s between two points in the invariants space yields a measure of the similitude of two different samples of a given object, thus a null distance would mean that two different samples produce exactly the same set of 7 invariant functions $\phi_i, i = 1, 2, \dots, 7$.

The distance between two points is measured with a generalization of the Pythagoras theorem:

$$d_s = \sqrt{\sum_{i=1}^7 (\phi_i^o - \phi_i)^2} \quad i = 1, 2, \dots, 7 \quad s = 1, 2, \dots, N_s - 1 \quad (13)$$

where ϕ_i^o is the set of invariants of the reference sample and ϕ_i is the set of invariants of any sample.

The mean distance $\langle d \rangle_n$ for object n is

$$\langle d \rangle_n = \frac{1}{N_s - 1} \sum_{s=1}^{N_s - 1} d_s \quad n = 1, 2, \dots, N_o \quad (14)$$

The average distance D for every object n in each method studied is given by:

$$D = \frac{\sum_{n=1}^{N_o} \langle d \rangle_n}{N_o} \quad (15)$$

After detecting the object edge, the improved (boundary) moments $i - \phi_i, i = 1, 2, \dots, 7$

were computed by two different methods, in the first, the edge pixels were taken into account by walking along the object boundary in no particular direction, being this a rather slow process since it is necessary to search in the neighbourhood surrounding every pixel in order to find its nearest neighbour, this procedure would fail if the object boundary presented gaps.

In the second method the image space was simply swept top-down and right-left, whenever an edge pixel was met it is considered in the computations, this process is very simple and quick since there is no particular edge sequence to maintain.

When computing both, massive and boundary moments the set of invariants (equations (4)) was used,

for the massive case the scaling factor was γ in equation (3), whereas for the boundary case the factor was α in equation (12).

The research included hollowed objects, in this case, objects with up to two hollows were used and their massive and boundary moments were computed. The massive moments were evaluated as usual by sweeping the image space.

When evaluating the improved moments by walking along the boundary, every object contour was tracked down separately (in no particular direction) and its invariant moments were computed, the object boundary invariants were the sum of these contour

moments. For the boundary moments by sweeping the image space, the pixels in the inner and outer boundaries were considered for computations as they were met, this is in no particular order, just as a chunk of pixels.

In tables (1), (2) and (3), $i - \phi_i$ stands for the improved moments, ϕ_i , for the traditional moments, W appears whenever the moments refer to those computed by walking along the boundary, S appears if the moments are related to those computed by sweeping the image space.

Tables 1 and 2 display the experimental results obtained for two of the sixteen objects used in the study, the position, orientation and size of the objects are random; each of the six RTS samples was evaluated with the three methods being investigated, thus every object has three associated sub-tables within each table.

In every sub-table each 7-element column represents the coordinates of a point in the hepta-dimensional invariants space. The first column in each sub-table was chosen as the reference for the other five columns in that sub-table.

In the case of non-hollowed objects it was experimentally found that the evaluation of the boundary moments with the two methods studied produced exactly the same numerical values, this was expected because in both cases it is the very same set of pixels that is being considered.

In the case of hollowed objects, the values resulting from the two ways of evaluating the boundary invariants were different, this was also expected, since when sweeping the image space, pixels from inner and outer contours are considered together as a single chunk and so a unique centroid is computed for them all; when walking along the boundaries, every object contour is associated to its particular centroid, its moments are computed with respect to this particular centroid and the definitive object moments result from the addition of these contour moments.

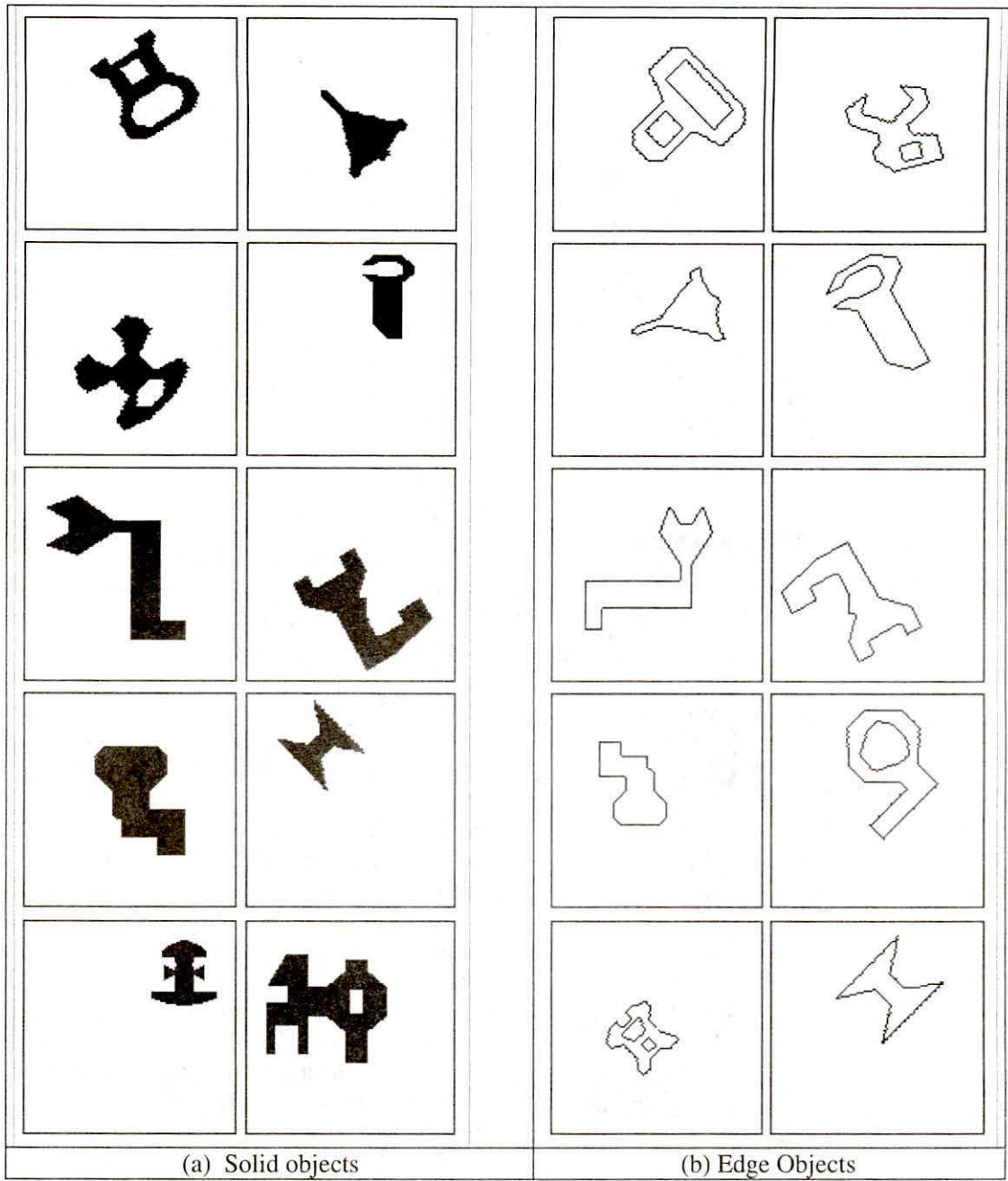


Fig. 1. Some RTS instances of some of the computer synthesized objects used in the experiments

TABLE I
EXPERIMENTAL VALUES FOR A HOLLOWED OBJECT

RTS Invariant function table						
Object : Hollowed Wrench (hollowed)						
	ϕ_i : massive moments			$i - \phi_i$: improved moments		
Rotation	45°	25°	-140°	-133°	-125°	23°
Size	80%	75%	85%	78%	50%	65%
ϕ_1 S	1.45	1.44	1.44	1.46	1.47	1.44
ϕ_2 S	10.53	9.21	11.14	9.79	11.85	13.64
ϕ_3 S	8.48	8.51	8.97	8.70	9.40	8.12
ϕ_4 S	12.25	10.51	10.86	10.40	13.70	10.99
ϕ_5 S	23.06	20.04	22.54	22.03	25.77	20.57
ϕ_6 S	17.61	15.88	16.53	15.31	20.02	17.96
ϕ_7 S	22.87	21.44	20.80	19.97	25.46	22.15
$i - \phi_1$ W	3.01	3.08	3.06	3.03	3.04	3.11
$i - \phi_2$ W	9.95	10.96	10.84	10.61	10.69	10.83
$i - \phi_3$ W	14.04	14.07	14.26	14.71	14.84	14.35
$i - \phi_4$ W	16.36	15.11	15.20	15.13	14.85	14.24
$i - \phi_5$ W	32.16	32.15	30.26	31.31	32.13	29.69
$i - \phi_6$ W	21.74	22.86	24.00	21.91	20.72	19.73
$i - \phi_7$ W	33.87	29.97	31.24	30.87	30.01	28.72
$i - \phi_1$ S	4.69	4.73	4.73	4.67	4.73	4.78
$i - \phi_2$ S	15.21	14.76	15.24	14.88	14.76	14.56
$i - \phi_3$ S	19.19	18.81	19.76	19.08	20.08	18.86
$i - \phi_4$ S	20.34	19.17	20.44	19.70	20.60	20.41
$i - \phi_5$ S	40.23	41.19	40.55	40.50	41.62	40.04
$i - \phi_6$ S	28.08	26.93	28.91	29.23	28.23	27.70
$i - \phi_7$ S	40.82	38.16	42.96	39.12	41.09	43.08
In every case the object location is random						
Since this is a hollowed object, then $i - \phi_i$ W is different from $i - \phi_i$ S						
All values are $-\ln(\text{abs}(\phi_i))$						

TABLE II
EXPERIMENTAL VALUES FOR A NON-HOLLOWED OBJECT

RTS Invariant function table						
Object : L-shaped wrench (non-hollowed)						
	ϕ_i : massive moments			$i - \phi_i$: improved moments		
Rotation	-33°	-145°	-27°	40°	-45°	80°
Size	75%	100%	60%	80%	110%	50%
ϕ_1 S	1.31	1.31	1.26	1.34	1.30	1.32
ϕ_2 S	3.72	3.71	3.56	3.82	3.70	3.83
ϕ_3 S	6.51	6.49	5.80	6.10	6.34	5.32
ϕ_4 S	8.06	8.65	7.60	7.80	8.71	7.11
ϕ_5 S	16.17	16.23	17.17	18.33	16.58	13.91
ϕ_6 S	9.95	10.81	11.07	11.55	10.57	9.54
ϕ_7 S	15.44	18.18	14.31	14.75	16.59	13.52
$i - \phi_1$ W	4.52	4.50	4.51	4.40	4.37	4.51
$i - \phi_2$ W	10.54	10.48	10.40	10.30	10.18	10.47
$i - \phi_3$ W	15.97	16.20	15.54	15.78	15.83	15.13
$i - \phi_4$ W	16.85	17.50	17.16	17.00	17.21	17.19
$i - \phi_5$ W	39.98	34.61	33.69	33.80	33.91	33.50
$i - \phi_6$ W	22.83	22.82	22.37	22.49	22.37	22.72
$i - \phi_7$ W	33.26	34.82	34.13	33.67	34.36	34.01
$i - \phi_1$ S	4.52	4.50	4.51	4.40	4.37	4.51
$i - \phi_2$ S	10.54	10.48	10.40	10.30	10.18	10.47
$i - \phi_3$ S	15.97	16.20	15.54	15.78	15.83	15.13
$i - \phi_4$ S	16.85	17.50	17.16	17.00	17.21	17.19
$i - \phi_5$ S	39.98	34.61	33.69	33.80	33.91	33.50
$i - \phi_6$ S	22.83	22.82	22.37	22.49	22.37	22.72
$i - \phi_7$ S	33.26	34.82	34.13	33.67	34.36	34.01
In every case the object location is random						
Since this is a non-hollowed object, then $i - \phi_i$ W is equal to $i - \phi_i$ S						
All values are $-\ln(\text{abs}(\phi_i))$						

Table 3 displays the experimental average distances D for the $N_o = 16$ objects (16 objects, 6 samples per object) investigated, from these 16 objects, 8 were hollowed and the other 8 non-hollowed. The resulting average distances D for the hollowed objects (identified 1 to 8 in table 3) are :

$$i - \phi_i \ W \quad D = 3.77, \text{ after normalizing: } D = 1.00 \quad (16)$$

$$i - \phi_i \ S \quad D = 3.28, \text{ after normalizing: } D = 0.87 \quad (17)$$

$$\phi_i \ S \quad D = 3.19, \text{ after normalizing: } D = 0.84 \quad (18)$$

the average distances D for the non-hollowed objects (9 to 16 in table 3) resulted

$$i - \phi_i \ W \quad D = 3.36, \text{ after normalizing: } D = 1.00 \quad (19)$$

$$i - \phi_i \ S \quad D = 3.36, \text{ after normalizing: } D = 1.00..(20)$$

$$\phi_i \ S \quad D = 3.22, \text{ after normalizing: } D = 0.95..(22)$$

the total average distances for the 16 objects are:

$$i - \phi_i \ W \quad D = 3.57, \text{ after normalizing: } D = 1.00 \quad (23)$$

$$i - \phi_i \ S \quad D = 3.32, \text{ after normalizing: } D = 0.92 \quad (24)$$

$$\phi_i \ S \quad D = 3.20, \text{ after normalizing: } D = 0.89 \quad (25)$$

From the total average distances above it can be seen that in general it is more convenient to compute the boundary moments by simply sweeping the image space instead of carrying out edge-tracing.

It can also be seen from the results that in the case of non-hollowed objects the distances in the case of boundary moments are close enough to those corresponding to the massive moments --which are being taken as a reference for this research-- this means that computing the boundary moments by sweeping the image space implies a reduction in computer time and computational complexity and enough accurateness.

When computing the boundary moments of hollowed objects, the resulting values suggest that image space sweeping is more practical than object edge-tracing. The fact that the resulting values are close to those of the reference massive invariants, suggest that the method proposed in this paper to perform pattern classification of hollowed objects achieves its mission satisfactorily.

TABLE III
AVERAGE DISTANCES, D

Object	Invariant Moments D		
	$\phi_i \ S$	$i - \phi_i \ S$	$i - \phi_i \ W$
1	3.021	2.967	3.775
2	4.157	2.416	4.592
3	4.340	4.070	2.813
4	1.052	3.881	6.395
5	2.375	3.115	2.506
6	5.776	3.387	4.244
7	2.074	2.015	3.050
8	2.707	4.368	2.787
9	2.541	6.207	6.207
10	7.411	4.201	4.201
11	2.652	4.605	4.605
12	2.289	2.641	2.641
13	3.847	2.751	2.751
14	1.462	2.148	2.148
15	1.876	1.581	1.581
16	3.666	2.756	2.756
Average	3.20	3.32	3.57

Table 3: Average Distances, D
Average distances D for the 16 objects used in the experiment. Objects from 1 to 8 are hollowed, from 9 to 16 are non hollowed

ϕ_i : Massive Moments
 $i - \phi_i$: Boundary Moments

S : moments computed by sweeping image space
W : moments computed by walking along object boundary

Notice that the non-hollowed objects have
 $i - \phi_i \ S = \phi_i \ W$

VI. DISCUSSION OF RESULTS

A study of the improved (boundary) moments in noise-free image-space has been carried out in a frame of reference given by the traditional (massive) moments.

The boundary moments have been computed following two different methods, in

the first, the edge pixels were considered by walking along the object boundary, this is by edge-tracing, in the second method the pixels are taken into account as they are met when sweeping the image space, this implies no particular order. For the massive

moments the totality of the object pixels were considered as usual by just sweeping the image space.

It was found in the experiment that in the case of non-hollowed objects, the average distance D between different object samples is the least when computing the massive moments, a slightly larger distance is obtained with the boundary moments.

If the traditional massive moments are taken as a reference, it can be concluded that the Chen's boundary

moments perform quite well. This means that the boundary moments and the massive moments are practically equivalent concerning distances between objects, however in the case of the massive moments the computational complexity is $O(N^2)$ while in the boundary moments it is only $O(N)$.

It has been experimentally found that from the three methods studied, the most convenient is the computation of the boundary moments by sweeping the image space. This conclusion is based on the fact that it is more economical to work with only the boundary pixels than with all the object pixels, and also in the fact that there is no need to compute the boundary moments by considering the pixel sequence, it is enough to compute them as they are met when sweeping the image space.

In order to compute the boundary moments of hollowed objects, the inner and outer edges were obtained for every RTS sample. In the case of the improved moments by walking along the boundaries, a walking was carried out in the inner and outer edges separately in no particular direction. The total boundary moments in this case were considered as the sum of the boundary moments of all the boundaries in the sample. In the case of boundary moments by sweeping the image space, the pixels of the inner and outer edges were considered simply as they were met, this is, in no particular sequence.

It was found that the method proposed here to evaluate the invariants of hollowed objects performs satisfactorily.

Besides the reduction in computer time and in computational complexity, an additional advantage of the improved moments by sweeping the image space is that the boundaries of the object do not need to be perfect, there can be any size gaps and the computations will not be significantly affected.

In the case of the improved moments by walking along the boundary, the presence of a gap may lead the computations to dire straits, so after obtaining the boundaries of a sample it would be necessary to pre-process so as to refill eventual gaps, a procedure that implies additional computations.

Even though the objects used in this research were computer synthesized and

consequently had very well defined boundaries, the application of the boundary

moments to real objects -which contours are not necessarily perfect- would have no problem seeing that when sweeping the image space the object contours do not need to be impeccable.

VII. CONCLUSION

It has been experimentally found that the computation of the Chen's improved moments yield practically the same average distances between invariants as those obtained by Hu's massive moments.

When computing the improved moments it is not necessary to use any chain code

representation of the object boundary, as suggested by Chen. Simply sweeping the image space produces exactly the same values that would be obtained by edge-tracing.

The improved moments have been applied to hollowed objects, the results demonstrate that this kind of objects may also be successfully classified with the boundary moment invariants.

VIII. ACKNOWLEDGEMENT

This research would not have been possible without the help of Miss Marlene Gonzalez Reyes, who created the computer synthesized objects, helped during the investigation, and typed the text and equations,

REFERENCES

- [1] Ming-Kuei Hu, Pattern recognition by moment invariants, Proceedings of the IRE, vol 49, page 1428, sept 1961
- [2] Ming-Kuei Hu, Visual Pattern recognition by moment invariants, IRE Transactions on information theory, 179-187, Feb-1962
- [3] Chaur-Chin Chen, Improved moment invariants for shape discrimination, Pattern recognition, Vol 26, No 5, 683-686, 1993
- [4] Javier Montenegro Joo, Invariant Boundary moments in Pattern Recognition. The method of C.C. Chen. Doctoral Qualification Exam (April 1994). Cybernetic Vision Research Group, Instituto de Física de Sao Carlos (IFSC), Dpto. de Física e Informática, Universidade de Sao Paulo (USP), Brazil.
- [5] Bing-Chen Li and Jun Shen, Fast computation of moment invariants. Pattern Recognition, Vol 24, No 8, 807-813, 1991
- [6] Mark H. Singer, A general approach to moment calculation for polygons and line segments. Pattern Recognition, Vol 26, No 7, 1019-1028, 1993
- [7] X.Y. Jiang and H.Bunke, Simple and fast

- computation of moments. Pattern recognition, Vol 24 No 8, 801-806, 1991
- [8] Jia-Guu Leu, Computing a shape's moments from its boundary. Pattern recognition, Vol 24 No 10, 949-957, 1991
- [9] S.Dudani, K.Breeding, R. McGhee, Aircraft identification by moment invariants. IEEE transactions on computers, vol C26, No 1, Jan 1977
- [10] Z. Mingfa, S. Hasani, S. Bhattarai, H. Singh, Pattern recognition with moment invariants on a machine vision system. Pattern Recognition Letters, Vol 19, 175-180, April 1989
- [11] C.W. Fu, J.C. Yen, S.Chang, Calculation of moment invariant via Hadamard transform. Pattern Recognition, Vol 26, No 2, 287-294, 1993
- [12] W. Wen, A. Lozzi, Recognition and inspection of manufactured parts using line moments of their boundaries. Pattern recognition, Vol 26, No 10, 1461-1471, 1993